[6] M. Kayahara, T. Nagakawa, K. Ueno, T. Ohta, T. Takeda, I. Miyazaki, An evaluation of radical resection for pancreatic cancer based on the mode of recurrence as determined by autopsy and diagnostic imaging, Cancer 72 (1993) 2118–2123.
[7] J.F. Griffin, S.R. Smalley, W. Jewell, J.C. Paradelo, R.D. Reymond, R.E. Hassanein, R.G. Evans, Patterns of failure after curative resection of pancreatic carcinoma, Cancer 66 (1990) 56–61.
[8] J. Westerdahl, A. Andren-Sandberg, I. Ihse, Recurrence of exocrine pancreatic cancer—local or hepatic? Hepatogastroenterology 40 (1993) 384–387.
[9] J.A. Cienfuegos, F.A. Manuel, Analysis of intraoperative radiotherapy for pancreatic carcinoma, Eur. J. Surg. Oncol. 26 (Suppl. A) (2000) S13–S15.
[10] W.F. Sindelar, T.J. Kinsella, Studies of intraoperative radiotherapy in carcinoma of the pancreas, Ann. Oncol. 10 (Suppl. 4) (1999) 226–230.
[11] A. Zerbi, V. Fossati, D. Parolini, M. Carlucci, G. Balzano, G. Bordogna, C. Staudacher, V. Di Carlo, Intraoperative radiation therapy adjuvant to resection in the treatment of pancreatic cancer, Cancer 73 (1994) 2930–2935.
[12] R.K. Jain, Barriers to drug delivery in solid tumors, Sci. Am. 271 (1994) 58–65.
[13] I.F. Tannock, Tumor physiology and drug resistance, Cancer Metastasis Rev. 20 (2001) 123–132.
[14] S.O. Hofer, G. Molema, R.A. Hermens, H.J. Wanebo, J.S. Reichner, H.J. Hoekstra, The effect of surgical wounding on tumour development, Eur. J. Surg. Oncol. 25 (1999) 231–243.
[15] S.O. Hofer, D. Shrayer, J.S. Reichner, H.J. Hoekstra, H.J. Wanebo, Wound-induced tumor progression: a probable role in recurrence after tumor resection, Arch. Surg. 133 (1998) 383–389.
[16] D.G. Baker, T.M. Masterson, R. Pace, W.C. Constable, H. Wanebo, The influence of the surgical wound on local tumor recurrence, Surgery 106 (1989) 525–532.
[17] M.N. Svendsen, K. Werther, H.J. Nielsen, P.E. Kristjansen, VEGF and tumour angiogenesis. Impact of surgery, wound healing, inflammation and blood transfusion, Scand. J. Gastroenterol. 37 (2002) 373–379.
[18] E.C. Kohn, L.A. Liotta, Molecular insights into cancer invasion: strategies for prevention and intervention, Cancer Res. 55 (1995) 1856–1862.
[19] A. Inoue, Y. Saijo, M. Maemondo, K. Gomi, Y. Tokue, Y. Kimura, M. Ebina, T. Kikuchi, T. Moriya, T. Nukiwa, Severe acute interstitial pneumonia and gefitinib, Lancet 361 (2003) 137–139.
[20] H. Okino, Y. Nakayama, M. Tanaka, T. Matsuda, In situ hydrogelation of photocurable gelatin and drug release, J. Biomed. Mater. Res. 59 (2002) 233–245.
[21] H. Okino, T. Manabe, M. Tanaka, T. Matsuda, Novel therapeutic strategy for prevention of malignant tumor recurrence after surgery: local delivery and prolonged release of adenovirus immobilized in photocured, tissue-adhesive gelatinous matrix, J. Biomed. Mater. Res. 66A (2003) 643–651.
[22] H. Okino, R. Maeyama, T. Manabe, T. Matsuda, M. Tanaka, Trans-tissue, sustained release of gemcitabine from photocured gelatin gel inhibits the growth of heterotopic human pancreatic tumor in nude mice, Clin. Cancer Res. 9 (2003) 5786–5793.
[23] T. Manabe, H. Okino, M. Tanaka, T. Matsuda, In situ-formed, tissue-adhesive co-gel composed of styrenated gelatin and styrenated antibody: potential use for local anti-cytokine antibody therapy on surgically resected tissues, Biomaterials 25 (2004) 5867–5873.
[24] T. Manabe, K. Mizumoto, E. Nagai, K. Matsumoto, T. Nakamura, T. Nukiwa, M. Tanaka, T. Matsuda, Cell-based protein delivery system for the inhibition of the growth of pancreatic cancer: NK4 gene-transduced oral mucosal epithelial cell sheet, Clin. Cancer Res. 9 (2003) 3158–3166.
[25] T. Manabe, H. Okino, R. Maeyama, M. Tanaka, T. Matsuda, The new infusion device for trans-tissue, sustained local delivery of Gemcitabine: potential use for the suppression of local recurrence of pancreatic cancer, J. Biomed. Mater. Res. (in press).
[26] W. Jiang, S. Hiscox, K. Matsumoto, T. Nakamura, Hepatocyte growth factor/scatter factor, its molecular, cellular and clinical implications in cancer, Crit. Rev. Oncol. Hematol. 29 (1999) 209–248.
[27] K. Matsumoto, K. Date, H. Ohmichi, T. Nakamura, Hepatocyte growth factor in lung morphogenesis and tumor invasion: role as a mediator in epithelium–mesenchyme and tumor–stroma interactions, Cancer Chemother. Pharmacol. 38 (1996) S42–S47.
[28] K. Date, K. Matsumoto, K. Kuba, H. Shimura, M. Tanaka, T. Nakamura, Inhibition of tumor growth and invasion by a four-kringle antagonist (HGF/NK4) for hepatocyte growth factor, Oncogene 17 (1998) 3045–3054.
[29] K. Date, K. Matsumoto, H. Shimura, T. Tanaka, T. Nakamura, HGF/NK4 is a specific antagonist for pleiotrophic actions of hepatocyte growth factor, FEBS Lett. 420 (1997) 1–6.
[30] N. Maehara, K. Matsumoto, K. Kuba, K. Mizumoto, M. Tanaka, T. Nakamura, NK4, a four-kringle antagonist of HGF, inhibits spreading and invasion of human pancreatic cancer cells, Br. J. Cancer 84 (2001) 864–873.
[31] K. Kuba, K. Matsumoto, K. Ohnishi, T. Shiratsuchi, M. Tanaka, T. Nakamura, Kringle 1–4 of hepatocyte growth factor inhibits proliferation and migration of human microvascular endothelial cells, Biochem. Biophys. Res. Commun. 279 (2000) 846–852.
[32] K. Kuba, K. Matsumoto, K. Date, H. Shimura, M. Tanaka, T. Nakamura, HGF/NK4, a four-kringle antagonist of hepatocyte growth factor, is an angiogenesis inhibitor that suppresses tumor growth and metastasis in mice, Cancer Res. 60 (2000) 6737–6743.
[33] L.W. Hertel, G.B. Boder, J.S. Kroin, S.M. Rinzel, G.A. Poore, G.C. Todd, G.B. Grindey, Evaluation of the antitumor activity of gemcitabine (2′,2′-difluoro-2′-deoxycytidine), Cancer Res. 50 (1990) 4417–4422.
[34] R.L. Merriman, L.W. Hertel, R.M. Schultz, P.J. Houghton, J.A. Houghton, P.G. Rutherford, L.R. Tanzer, G.B. Boder, G.B. Grindey, Comparison of the antitumor activity of gemcitabine and ara-C in a panel of human breast, colon, lung and pancreatic xenograft models, Invest. New Drugs 14 (1996) 243–247.

[35] V.W. Ruiz van Haperen, G. Veerman, P. Noordhuis, J.B. Vermorken, G.J. Peters, Concentration and time dependent growth inhibition and metabolism in vitro by 2′,2′-difluorodeoxycytidine (gemcitabine), Adv. Exp. Med. Biol. 309A (1991) 57–60.

[36] V.W. Ruiz van Haperen, G. Veerman, E. Boven, P. Noordhuis, J.B. Vermorken, G.J. Peters, Schedule dependence of sensitivity to 2′,2′-difluorodeoxycytidine (Gemcitabine) in relation to accumulation and retention of its triphosphate in solid tumour cell lines and solid tumours, Biochem. Pharmacol. 48 (1994) 1327–1339.

[37] G. Veerman, V.W. Ruiz van Haperen, J.B. Vermorken, P. Noordhuis, B.J. Braakhuis, H.M. Pinedo, G.J. Peters, Antitumor activity of prolonged as compared with bolus administration of 2′,2′-difluorodeoxycytidine in vivo against murine colon tumors, Cancer Chemother. Pharmacol. 38 (1996) 335–342.

[38] M. Kommann, U. Butzer, J. Blatter, H.G. Beger, K.H. Link, Pre-clinical evaluation of the activity of gemcitabine as a basis for regional chemotherapy of pancreatic and colorectal cancer, Eur. J. Surg. Oncol. 26 (2000) 583–587.

[39] C. Li, T. Sajili, Y. Nakayama, M. Fukui, T. Matsuda, Novel visible-light-induced photocurable tissue adhesive composed of multiply styrene-derivatized gelatin and poly(ethylene glycol) diacrylate, J. Biomed. Mater. Res. 66B (2003) 439–446.

[40] O. Ishikawa, H. Ohigashi, Y. Sasaki, H. Furukawa, T. Kabuto, M. Kameyama, S. Nakamori, M. Hiratsuka, S. Imaoka, Liver perfusion chemotherapy via both the hepatic artery and portal vein to prevent hepatic metastasis after extended pancreatectomy for adenocarcinoma of the pancreas, Am. J. Surg. 168 (1994) 361–364.

[41] O. Ishikawa, H. Ohigashi, S. Imaoka, Y. Sasaki, M. Kameyama, S. Nakamori, T. Kabuto, H. Furukawa, Regional chemotherapy to prevent hepatic metastasis after resection of pancreatic cancer, Hepatogastroenterology 44 (1997) 1541–1546.

[42] H.G. Beger, F. Gansauge, M.W. Buchler, K.H. Link, Intraarterial adjuvant chemotherapy after pancreaticoduodenectomy for pancreatic cancer: significant reduction in occurrence of liver metastasis, World J. Surg. 23 (1999) 946–949.

[43] H.G. Beger, K.H. Link, F. Gansauge, Adjuvant regional chemotherapy in advanced pancreatic cancer: results of a prospective study, Hepatogastroenterology 45 (1998) 638–643.

[44] C.M. Lee, T. Tanaka, T. Murai, M. Kondo, J. Kimura, W. Su, T. Kitagawa, T. Ito, H. Matsuda, M. Miyasaka, Novel chondroitin sulfate-binding cationic liposomes loaded with cisplatin efficiently suppress the local growth and liver metastasis of tumor cells in vivo, Cancer Res. 62 (2002) 4282–4288.

[45] T. Tamura, F. Fujita, M. Tanimoto, M. Koike, A. Suzuki, M. Fujita, Y. Horikiri, Y. Sakamoto, T. Suzuki, H. Yoshino, Antitumor effect of intraperitoneal administration of cisplatin-loaded microspheres to human tumor xenografted nude mice, J. Control. Release 80 (2002) 295–307.

[46] M. Lohr, F. Hummel, G. Faulmann, J. Ringel, R. Saller, J. Hain, W.H. Gunzburg, B. Salmons, Microencapsulated, CYP2B1-transfected cells activating ifosfamide at the site of the tumor: the magic bullets of the 21st century, Cancer Chemother. Pharmacol. 2002 (Suppl. 1) (2002) S21–S24.

[47] R.K. Jain, Barriers to drug delivery in solid tumors, Sci. Am. 271 (1) (1994) 42–49.

[48] R.K. Jain, Delivery of molecular medicine to solid tumors: lesson from in vivo imaging of gene expression and function, J. Control. Release 74 (1–3) (2001) 7–25.

Acute volume reduction with aortic valve replacement immediately improves ventricular mechanics in patients with aortic regurgitation

Shigeki Morita, MD
Yoshie Ochiai, MD
Yoshihisa Tanoue, MD
Manabu Hisahara, MD
Munetaka Masuda, MD
Hisataka Yasui, MD

Objectives: Few data have been available regarding the immediate response in ventricular mechanics to acute volume reduction caused by aortic valve replacement for aortic regurgitation.

Methods: We studied 9 patients in the operating room immediately before and after the institution of cardiopulmonary bypass. Left ventricular pressure and cross-sectional area (a surrogate of left ventricular volume) were measured with a catheter-tip manometer and a transesophageal echocardiographic system equipped with automated border-detection technology. Left ventricular pressure-area loops were constructed, and the caval occlusion method was used to obtain the slope of the end-systolic pressure-area relationship and the end-systolic area associated with 100 mm Hg. From the steady-state beats, stroke area was obtained by subtracting the minimum area from the maximum area. Effective arterial elastance, a measure of ventricular afterload, was calculated from end-systolic pressure, and stroke area as follows: effective arterial elastance equals end-systolic pressure divided by stroke area.

Results: Reductions in maximum area (21.0 ± 8.5 to 16.0 ± 6.8 cm^2 [SD])and minimum area (15.3 ± 8.4 to 12.0 ± 6.1 m^2) shifted the baseline pressure-area loops to the left. The slope of the end-systolic pressure-area relationship (11.6 ± 4.8 to 16.0 ± 7.5 mm Hg/cm^2) and afterload (effective arterial elastance, 17.9 ± 11.6 to 26.3 ± 16.4 mm Hg/cm^2) were increased, and the end-systolic area associated with 100 mm Hg was reduced (18.3 ± 10.0 to 13.7 ± 5.8 cm^2).

Conclusion: Correction of volume overload reduced preload (minimum area), shifted the end-systolic pressure-area relationship to the left (decreased end-systolic area), and improved ventricular contractility (increased slope of the end-systolic pressure-area relationship). The result indicated that acute volume reduction favorably influenced ventricular mechanical parameters immediately after the operation.

From the Department of Cardiovascular Surgery, Faculty of Medicine, Kyushu University, Fukuoka, Japan.

Received for publication June 27, 2002; revisions requested July 26, 2002; revisions received Sept 9, 2002; accepted for publication Sept 13, 2002.

Address for reprints: Shigeki Morita, MD, Department of Cardiovascular Surgery, Faculty of Medicine, Kyushu University, 3-1-1 Maidashi, Higashi-ku, Fukuoka 812-8582, Japan (E-mail: morita@heart.med.kyushu-u.ac.jp).

J Thorac Cardiovasc Surg 2003;125:283-9

0022-5223/2003 $30.00+0

doi:10.1067/mtc.2003.20

Improvement in ventricular function caused by load-reduction therapy is a well-established concept in the treatment of congestive heart failure. The immediate effect of acute load alteration on ventricular function is not clearly understood, however. In patients with aortic regurgitation (AR), the elimination of regurgitant volume by means of aortic valve replacement (AVR) causes significant reduction in left ventricular (LV) end-diastolic volume or preload.[1] In general, reduction in preload results in a decrease in blood pressure. Thus when preload is reduced, an improvement in contractility, an increase in afterload, or both should accompany the maintenance of adequate blood pressure.

There have been few data available, however, to show the restoration of LV contractility immediately after AVR in the operating room.

Accordingly, the current study was designed to elucidate the interrelationship among preload, afterload, and contractility immediately before and after AVR in patients with AR. For this purpose, we applied the framework of the LV pressure-volume relationship[2] and the concept of ventricle-afterload coupling.[3] We used transesophageal echocardiography (TEE) with the capability of automated border detection (ABD), which provided online output of the ventricular cavity area measurement. Because there is a close relationship between LV volume and short-axis cross-sectional area (CSA),[4,5] CSA has been used as a surrogate of LV volume. Combining LV pressure and CSA yields LV pressure-area loops, which could be used to apply the framework of LV pressure-volume relationship. With this approach, we measured end-systolic elastance (Ees; contractility) and effective arterial elastance (Ea; afterload) to elucidate the mechanism of the response of LV performance after AVR.

ACD

Patients and Methods

Nine male patients (age range, 38-74 years; median, 66 years) who underwent elective AVR for the correction of pure AR were studied in the operating room. LV ejection fraction (EF) measured by means of a preoperative catheterization study was normal (mean, 57% ± 10% [SD]), with increased end-diastolic volume index (236 ± 64 mL/m^2) and end-systolic volume index (114 ± 50 mL/m^2). LV end-diastolic pressure was moderately increased (17.5 ± 6.6 mm Hg), with a normal cardiac index (3.1 ± 0.9 L · min^{-1} · m^{-2}). All patients had grade 4/4 AR, except for 2 patients who had grade 3/4 AR. The study was approved by the institutional review board of the Faulty of Medicine, Kyushu University. Informed written consent was obtained from all patients. In the operating room a radial artery line was inserted after achievement of local anesthesia. After the induction of general anesthesia, a 7.5F thermodilution pulmonary artery catheter (model 93-A431H; Baxter Healthcare Corp, Irvine, Calif) was positioned through the right internal jugular vein. The heart was exposed through a median sternotomy and a longitudinal incision of the pericardium. Heparin was given, and arterial and venous cannulas were inserted and connected to a heart-lung machine. Tapes were passed around the superior and inferior venae cavae. A catheter-tipped manometer (MPC 350; Millar Instruments, Inc, Houston, Tex) or a fiber-optic catheter (Sentron, AC Roden, The Netherlands) was inserted through the stab wound of the left ventricle or through the right upper pulmonary vein through the mitral valve. A 5-MHz omniplane TEE probe (model HP 21362C; Hewlett-Packard, Andover, Mass) that had been inserted after the induction of anesthesia was positioned to obtain a cross-sectional view of the left ventricle at the level of the midpapillary muscle. Echocardiographic images were acquired by using a Hewlett-Packard Sonos 2500 echocardiographic system (model M2406A, Hewlett-Packard) with an ABD capability. A region of interest was drawn manually immediately beyond the LV endocardial border to exclude low-density ultrasound signals that might appear within the lateral myocardium. Once the image had been established, the same region of interest and the gain setting were maintained throughout the protocol for each patient.

Protocol

After the adequate placement of the TEE probe, thermodilution cardiac output was measured, and LV pressure and CSA were recorded simultaneously to obtain steady-state baseline data. Using the tape passed around the inferior vena cava, we occluded the cava to obtain multiple beats with different preload. The quality of the recorded data was checked immediately. When satisfactory recordings were obtained, cardiopulmonary bypass was instituted, and a routine AVR was performed. The same measurement was performed within 5 minutes after the discontinuation of cardiopulmonary bypass before removing the cannulas and neutralizing heparin. The postcardiopulmonary bypass measurement took no more than 10 minutes.

Data Acquisition and Analysis

Pressures of the left ventricle, the radial artery, the pulmonary artery, and the right atrium along with lead II echocardiographic signals and LV area signals from the echocardiography machine were digitized online at 200 Hz with an analog-to-digital converter (Mac Lab System; AD Instruments, Ltd, Dunedin North, New Zealand). These signals were recorded on a hard disk of a laptop computer (Macintosh Power Book 550C; Apple Computer, Inc, Cupertino, Calif), and LV pressure and area signals were plotted to display pressure-area loops. There is a delay in LV area signal because of the signal processing. Our preliminary study directly comparing ventricular volume obtained from a conductance catheter and area signal from ABD showed that the delay was 40 ms. Accordingly, we advanced the LV area signal by 40 ms in all patients.

From the steady-state beats, maximal CSA (Amax) and minimal CSA (Amin) were obtained. Stroke area (SA; SA = Amax − Amin) and fractional area change (FAC; FAC = SA/Amax) were calculated. SA and FAC were used as the echocardiographic equivalents of stroke volume and EF, respectively.

Contractility was assessed by using 3 indices: (1) Ees,[2,6] which is the slope of the end-systolic pressure-area relationship (ESPAR); (2) the slope of the stroke work (SW) end-diastolic area (Aed) relationship (Msw)[7]; and (3) the ratio of maximal dp/dt to Aed (dp/dt$_{max}$ to Aed ratio).[8] For ESPAR and SW-Amax relationships, area axis intercepts were measured as well (Ao,es and Ao,sw, respectively). The area associated with the LV end-systolic pressure (Pes) of 100 mm Hg was calculated to determine the position of the ESPAR in the operating range as follows:

$$A_{100},es = Ao + 100/Ees \quad (1)$$

Similarly, the position of the SW-Aed in the operating range was determined by calculating A_{500},sw. Diastolic function was assessed by fitting the end-diastolic pressure-area relationship to exponential function, and the stiffness constant (β) was calculated as previously reported.[9] By using the above obtained exponential function, the area that provides the end-diastolic pressure of 8 mm Hg was calculated (A_8,ed).

The effective arterial elastance, Ea, a measure of LV afterload, was calculated as Pes/SA,[3] and the ventricle-afterload coupling

TABLE 1. Conventional hemodynamic data

	HR (min^{-1})	Prad,s (mm Hg)	Prad,d (mm Hg)	Prad,m (mm Hg)	CI ($L \cdot min^{-1} \cdot m^{-2}$)	LAP (mm Hg)	RAP (mm Hg)	SVRI ($dynes \cdot s^{-1} \cdot cm^{-5} \cdot m^{-2}$)
Before	73 ± 14	105 ± 10	38 ± 9	61 ± 9	2.7 ± 0.8	8.2 ± 2.0	4.4 ± 0.8	1913 ± 950
After	90 ± 19	93 ± 15	55 ± 13	68 ± 15	2.8 ± 0.8	7.0 ± 2.1	4.5 ± 1.2	1922 ± 693
P value	.011	.169	.027	.316	.781	.243	.851	.987

All values are expressed as means ± SD. *HR,* Heart rate; *Prad,s,* systolic radial artery pressure; *Prad,d,* diastolic radial artery pressure; *Prad,m,* mean radial artery pressure; *CI,* cardiac index; *LAP,* left atrial pressure; *RAP,* right atrial pressure; *SVRI,* systemic vascular resistance index.

ratio was obtained (Ea/Ees). In addition, the systemic vascular resistance index, a standard parameter of afterload, was calculated as follows:

$$([Mean\ arterial\ pressure - Right\ atrial\ pressure]/Cardiac\ index) \times 80 \quad (2)$$

The total mechanical energy generated by means of ventricular contraction defined by pressure-volume area (PVA)[10] was obtained as the area circumscribed by the end-systolic trajectory of the pressure-area loop, the end-systolic pressure-area line, and the end-diastolic pressure-area relationship. SW was calculated as the area inside the pressure-area loop. The efficiency of energy transfer from PVA to SW was evaluated as SW/PVA.

Statistics

Results are presented as means ± SD. A paired *t* test was performed to compare the variables before and after AVR.

Results

All 9 patients underwent AVR with mechanical prostheses (Carbomedics, Austin, Tex). The ischemic time ranged from 31 to 124 minutes, with a median value of 61 minutes. No patients received inotropic or vasodilating agents. There were no study-related complications, and all patients were discharged with an uneventful postoperative course.

There was no change in conventional hemodynamic variables after AVR, except for increased heart rate and higher diastolic radial artery pressure (Table 1). During the vena caval occlusion, there was no significant increase in heart rate, but heart rate tended to increase after the release of occlusion. This phenomenon indicated that caval occlusion did cause a baroreflex response, but the reflex was not prompt enough to influence the data during vena caval occlusion. Representative LV pressure-area loops before and after AVR are shown in Figure 1. Because of the reduction in Amax and Amin, baseline loops were shifted to the left. The ESPAR also shifted to the left with an increase in the slope (Ees). It can be appreciated that there was no isovolumic relaxation phase caused by AR. The pressure at the start of ejection (the right shoulder of the loop) was lower before AVR, probably because of low diastolic arterial pressure. Ea, a parameter of afterload, was increased after AVR. Variables obtained from the baseline loops in all patients are summarized in Table 2. There was a 24% reduction in Amax and a 22% decrease in Amin. SA was reduced by 31%. There was no change in FAC. The parameters of contractility are shown in Table 3. There was an increase in Ees by 38%, with no difference in the area axis intercept (Ao,es). A decrease in A_{100},es indicated that the operating points of the ESPAR were shifted to the left after AVR. The slope of the SW-Aed relationship was reduced by 31% (marginally significant, $P = .136$), which usually indicated reduced contractility. The reason for the decrease in Msw will be given in the "Discussion" section. A parameter fairly independent of preload (dp/dt_{max} to Aed ratio)[8] was increased by 59%. As shown in Table 4, Ea was increased by 46%. Because there were similar increases in Ea and Ees, there was no significant change in the coupling ratio Ea/Ees. Because of the reduction in LV volume, PVA was reduced by 24%, although the difference was marginal ($P = .128$). The reduction in SW was 42%. There was no change in SW/PVA. No difference was found in the parameters of diastolic function (β and A_8,ed).

Discussion

We found that in patients with pure AR, there was an improvement in contractile function, reduction in both preload and mechanical LV work, and increase in ventricular afterload immediately after AVR. We used a previously validated method[4,5,11] of using the cross-sectional cavity area, obtained by means of echocardiography, as a surrogate for volume, which allowed us to apply the framework of LV pressure-volume relationship in the operating room. To the best of our knowledge, this is the first study to demonstrate improvement in contractile function immediately after AVR by using the framework of the pressure-volume relationship in patients with AR.

There was a significant improvement in ventricular contractility evidenced by the increase in the slope (Ees) and the leftward shift (decrease in A_{100},es) of the ESPAR. One might argue that in the presence of reduced LV volume after AVR, Ees was falsely high because there is an inverse relationship between Ees and the size of the ventricle. However, this might not be the case. First, this is because the observation was limited to the same subject (same heart) and we were not comparing Ees among the subjects with

ACD

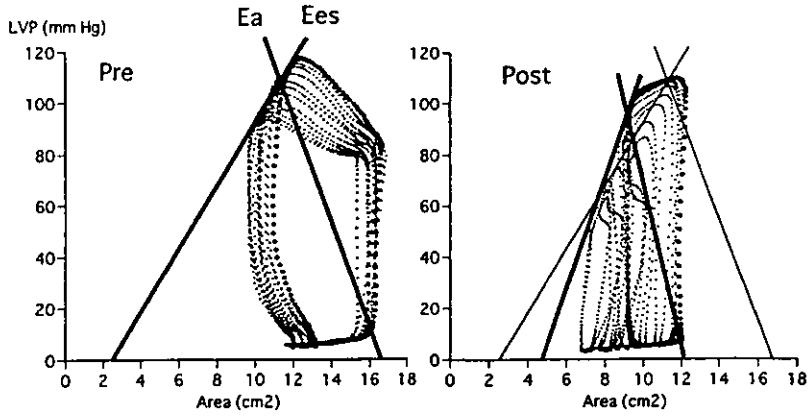

Figure 1. Representative pressure-area loops before *(left panel)* and after *(right panel)* AVR. Baseline loops are shown by *large dots*, and loops during caval occlusion are shown by *small dots*. *Solid lines* are the lines of Ees and Ea. In the right panel *thin lines* are the lines of Ees and Ea before AVR. *LVP*, LV pressure.

TABLE 2. Variables obtained from baseline loops

	Ped (mm Hg)	Pes (mm Hg)	Amax (cm^2)	Amin (cm^2)	SA (cm^2)	FAC (%)	dp/dt_{max} (mm Hg/s)
Before	7.6 ± 1.6	88.7 ± 17.0	21.0 ± 8.5	15.3 ± 8.4	5.8 ± 2.0	30.4 ± 14.0	723 ± 228
After	7.3 ± 1.4	89.8 ± 22.5	16.0 ± 6.8	12.0 ± 6.1	4.0 ± 1.4	26.8 ± 9.1	850 ± 344
P value	.829	.899	.013	.046	.022	.276	.280

Ped, LV end-diastolic pressure; dp/dt_{max}, maximum value of the first derivative of LV pressure.

TABLE 3. Parameters of contractility

	Ees ($mm\ Hg/cm^2$)	Ao,es (cm^2)	A_{100},es (cm^2)	Msw (mm Hg)	Ao,sw (cm^2)	A_{500},sw (cm^2)	dp/dt_{max}/Aed ($mm\ Hg \cdot s^{-1} \cdot cm^{-2}$)
Before	11.6 ± 4.8	6.6 ± 5.7	18.3 ± 10.0	68.9 ± 14.1	13.5 ± 8.0	21.0 ± 8.0	41.3 ± 19.2
After	16.0 ± 7.5	5.7 ± 3.9	13.7 ± 5.8	49.8 ± 30.9	9.8 ± 4.5	22.2 ± 6.7	65.5 ± 44.5
P value	.035	.561	.037	.139	.035	.431	.040

Ao,es, Area-axis intercept of the end systolic pressure area relationships; A_{100},es, end-systolic area that gives the Pes of 100 mm Hg; Ao,sw, area-axis intercept of the SW-Aed relationships; A_{500},sw, area that gives the SW of 500 mm Hg.cm^2; dp/dt_{max}, maximum value of the first derivative of LV pressure.

TABLE 4. Parameters and variables of afterload, energetics, and diastolic function

	Ea ($mm\ Hg/cm^2$)	Ea/Ees	SW ($mm\ Hg.cm^2$)	PVA ($mm\ Hg.cm^2$)	SW/PVA	β	$A_\beta$ed (cm^2)
Before	17.9 ± 11.6	1.98 ± 1.72	447 ± 135	1082 ± 430	0.45 ± 0.16	0.14 ± 0.07	19.9 ± 10.1
After	26.3 ± 16.4	1.89 ± 1.38	258 ± 103	820 ± 458	0.34 ± 0.12	0.15 ± 0.11	16.7 ± 6.9
P value	.010	.720	.003	.128	.030	.704	.271

β, Stiffness constant of the end-diastolic pressure-area relationship; $A_\beta$ed, area associated with an end-diastolic pressure of 8 mm Hg.

different ventricular sizes. Second, this is because the increase in Ees and the leftward shift of the ESPAR did not accompany the alteration in diastolic pressure-area relationship. In general, a smaller heart shows higher Ees with stiffer diastolic function (smaller end-diastolic volume with a given end-diastolic pressure), which results in reduced overall pump function (smaller stroke volume). In our patient there was no change in diastolic function after AVR. Thus the leftward shift of the ESPAR definitely implied improvement in overall LV pump function. Our view was

supported by the improvement in the dp/dt_{max} to Amax ratio, another parameter of contractility, which is less sensitive to ventricular size or preload.[8]

The reduction in Msw, which is called preload recruitable stroke work, generally implies a decrease in contractility.[7] In our patients reduced Msw could be explained by altered ejection physiology in AR. When forward stroke volume is maintained in AR, LV stroke volume (the difference between end-diastolic and end-systolic volume) is increased because of the excessive regurgitant volume. The low diastolic blood pressure in AR causes the increased rate and volume of blood flow into the aorta during early systole to midsystole,[12] which results in wide pulse pressure but relatively normal end-systolic pressure. Early augmented ejection with increased LV stroke volume might imply reduced ejection load to the ventricle. This was indeed the case in our study because Ea was low before AVR and was increased after the operation. Ea is a parameter of ventricular afterload, which represents both pulsatile and static load to the ventricle,[3,13] and is used to evaluate the interaction between the ventricle and the ejection load. According to Sunagawa and colleagues,[3] SW is determined by the interaction among Ea, Ees, and end-diastolic volume. The linearity and load independence of preload recruitable SW is considered to be due to the fact that SW is fairly constant when the value of Ea is in the normal range.[14] In our patients, however, there was a greater than 40% increase in Ea after AVR, which resulted in a decrease in SW. Because it has been shown that SW decreases when Ea is increased,[15] it is conceivable that reduced Msw in our patients was due to the increase in Ea (below normal preoperatively returning to normal) after AVR.

Several previous studies support our view. Gaynor and coworkers[16] performed an experimental study showing the increase of Msw after the creation of AR. Although they did not provide Ea data, their pressure-volume loops clearly demonstrated a widening of the loop (increased stroke volume) with no significant change in height (no change in Pes), indicating decreased Ea after the creation of AR. In another study Starling and colleagues[17] made an interesting observation in patients who underwent AVR for AR. They measured maximal elastance (Emax; a term almost identical to Ees[6]) before AVR and found that those who had had normal EF and mildly decreased Emax (group I) showed no change in EF (61% to 63%), those who had had mildly decreased EF and moderately decreased Emax (group II) showed an improvement in EF (50% to 64%), and those who had had severely decreased EF and Emax (group III) showed a further decrease in EF (35% to 30%). Why was there a decrease in EF in group III? The researchers did not perform a postoperative pressure-volume study, but it is highly conceivable that the postoperative Emax value improved in all patients because there was a significant reduction in end-systolic volume in all patients. A further decrease in EF despite an increase in Emax in group III patients could be explained by the fact that the degree of increase in Ea after AVR was largest in these patients. The values of Ea calculated from their preoperative stroke volume and LV pressure data were 1.45, 0.84, and 0.58 mm Hg/mL, respectively, for groups I, II, and III. Thus normalization of Ea by AVR must have caused the largest increase in Ea for group III patients, which caused a decrease in EF. These data, including ours, indicate a close inverse relationship between the severity of AR and Ea.

In general, LV function improves after AVR in patients with AR.[1,18,19] Most previous reports used EF to estimate contractility. There has been no post-AVR study that used Ees as the parameter of contractility under the framework of the pressure-volume relationship. The current study is also unique in elucidating load-independent ventricular function immediately after the discontinuation of cardiopulmonary bypass. Although load-independent indices are not available weeks or months after surgical intervention, it is highly conceivable that the improved contractile function observed in our study might continue to be improved because LV end-systolic volume is reported to be significantly reduced 3 to 6 months after AVR.[17] Because Pes, which is very close to mean arterial pressure, is fairly constant, smaller volume with similar end-systolic pressure indicates that Ees is increased weeks or months after AVR.

The mechanism of the immediate recovery of contractility after AVR in our study is not clear. Reduction of LV volume caused a decrease in the work load of the left ventricle, with an increase in energy supply (higher diastolic blood pressure implying better myocardial perfusion). The improvement in the energy supply and demand ratio might have had a favorable effect in causing contractility enhancement. At the sarcomere level, reduction in volume after AVR, which caused the decrease in sarcomere length, might have optimized the operational length of the sarcomere. In terms of LV wall stress, the decrease in LV diameter after AVR should reduce the LV wall stress, which would work favorably for LV mechanics. A similar mechanism for explaining the improvement in ventricular volume or wall stress reduction operations (such as the Batista operation) or the Myosplint procedure has been advocated.[20,21] Our results also might explain the mechanism of improved ventricular function observed after LV assist device implantation in some patients.[22] Further study is warranted to elucidate the exact mechanism.

One might argue that these findings could be the result of cardiopulmonary bypass and not AVR. This might not be the case, however, because our preliminary results studying patients with aortic stenosis showed exactly the opposite response after AVR (ie, reduction in both Ees and Ea). Combining our current results and the described unpub-

lished data, we might safely assume that the changes in loading condition has a significant influence on contractile function and that the findings obtained in our current study were the result of AVR and not the result of cardiopulmonary bypass.

Ees is the slope of the ESPAR, which is assumed to be a load-insensitive parameter of contractility.[2] In addition to the size-dependent nature of the Ees, which has been already discussed in this article, the limitation of Ees includes curvilinearity of ESPAR when the contractility is either markedly increased or severely decreased.[21] Among the parameters we used, the decrease in A_{100},es indicated shift to the left of ESPAR, which is independent of curvilinearity. In addition, the dp/dt_{max} to Aed ratio, another parameter of contractility that is assumed to be independent of loading conditions, was increased. These results support the conclusion of increased contractility after AVR.

Heart rate has positive effects on both Ees[23] and Ea.[13] The increases in Ees and Ea might partly be due to the increase in heart rate observed in our patients. However, the increases observed in our patients (38% increase in Ees and 47% increase in Ea) were larger than the predicted increases in Ees of 13%[23] and Ea of 23%,[13] provided that the increase in heart rate from 73 to 90 beats/min was the only contributing factor for the increases in Ees and Ees. We thus assume that replacing the leaking valve with a competent valve was the major cause of the increases in Ees and Ea in our patients.

The approach of using LV cavity area as a surrogate for volume has been validated.[4,5,11] We performed preliminary animal studies comparing CSA and LV volume measured either with a conductance catheter or with an isolated canine ejecting heart preparation. Both studies showed extremely linear correlation between the area and volume. We also found that the area signal was delayed for 40 ms. On the basis of this finding, area signal in the present study was advanced for 40 ms. Although previous validation studies support the use of area as a surrogate for volume, no validation study has been performed in the dilated heart, such as in our patients. In addition, rotational or swinging movement of the heart during one cardiac cycle might alter the relationship between cross-sectional cavity area and ventricular volume. Further investigation, such as that with 3-dimensional reconstruction of the LV cavity, should be performed to validate the methodology for applying this technique for hearts with abnormal geometry and movement.

The majority of our patients had normal EF preoperatively. Thus our results might not be able to be extrapolated to patients with AR with decreased EF. However, the results for patients with AR with low EF in the literature are encouraging,[18,19] and accordingly, further study is warranted to elucidate the mechanism of improvement in the LV function in patients with AR with the most decreased ventricular function.

We thank Dr Noriya Taki, the director of The Institute for Medical Statistics, for his work as a consultant statistician.

References

1. Krayenbuehl HP, Hess OM, Monrad ES, Schneider J, Mall G, Turina M. Left ventricular myocardial structure in aortic valve disease before, intermediate and late after aortic valve replacement. *Circulation.* 1989;79:744-55.
2. Sagawa K, Suga H, Shoukas AA, Bakalar KM. End-systolic pressure/volume ratio: a new index of ventricular contractility. *Am J Cardiol.* 1977;40:748-53.
3. Sunagawa K, Maughan WL, Burkhoff D, Sagawa K. Left ventricular interaction with arterial load studied in isolated canine ventricle. *Am J Physiol.* 1983;245:H773-80.
4. Gorcsan J 3rd, Gaisior TA, Mandarino WA, Denault LG, Hattler BG, Pinsky MR. On-line estimation of changes in left ventricular stroke volume by transesophageal echocardiographic automated border detection in patients undergoing coronary artery bypass grafting. *Am J Cardiol.* 1993;72:721-7.
5. Gorcsan J 3rd, Lazar JM, Schulman DS, Follansbee WP. Comparison of left ventricular function by echocardiographic automated border detection and by radionuclide ejecition fraction. *Am J Cardiol.* 1993; 72:810-5.
6. Kass DA, Maughan WL. From "Emax" to pressure-volume relations: a broader view. *Circulation.* 1988;78:736-43.
7. Glower DD, Spratt JA, Snow ND, Kabas JS, Davis JW, Olsen CO, et al. Linearity of the Frank-Starling relationship in the intact heart: the concept of preload recruitable stroke work. *Circulation.* 1985;71:994-1009.
8. Feldman MD, Pak PH, Wu CC, Haber HL, Heesch CM, Bergin JD, et al. Acute cardiovascular effects of OPC-18790 in patients with congestive heart failure: time and dose-dependence analysis based on pressure-volume relations. *Circulation.* 1996;93:474-83.
9. Gaash WH, Battle WE, Obolor AA, Banas JS Jr, Levine HJ. Left ventricular stress and compliance in man. With special reference to normalized ventricular function curves. *Circulation.* 1972;45:746-62.
10. Suga H. Ventricular energetics. *Physiol Rev.* 1990;70:247-77.
11. Ochiai Y, Morita S, Tanoue Y, Kawachi Y, Tominaga R, Yasui H. Effects of amrinone, a phophodiesterase inhibitor on right ventricular/arterial coupling immediately after cardiac operations. *J Thorac Cardiovasc Surg.* 1998;116:139-47.
12. Borow KM, Marcus RH. Aortic regurgitation: the need for an integrated physiological approach. *J Am Coll Cardiol.* 1991;17:898-900.
13. Kelly RP, Ting CT, Yang TM, Maughan WL, Chang MS, Kass DA. Effective arterial elastance as index of arterial vascular load in humans. *Circulation.* 1992;86:513-21.
14. Kass DA, Maughan WL, Guo ZM, Kono A, Sunagawa K, Sagawa K. Comparative influence of load versus inotropic states on indexes of ventricular contractility: experimental and theoretical analysis based on pressure-volume relationships. *Circulation.* 1987;76: 1422-36.
15. Sunagawa K, Maughan WL, Sagawa K. Optimal arterial resistance for the maximal stroke work studied in isolated canine left ventricle. *Circ Res.* 1984;54:595-602.
16. Gaynor JW, Feneley MP, Gall SA Jr, Savitt MA, Silvestry SC, Davis JW, et al. Left ventricular adaptation to aortic regurgitation in conscious dogs. *J Thorac Cardiovasc Surg.* 1997;113:149-58.
17. Starling MR, Kirsh MM, Montgomery DG, Gross MD. Mechanisms for left ventricular systolic dysfunction in aortic regurgitation: importance for predicting the functional response to aortic valve replacement. *J Am Coll Cardiol.* 1991;17:887-97.

18. Carabello BA, Usher BW, Hendrix GH, Assey ME, Crawford FA, Leman RB. Predictors of outcome for aortic valve replacement in patients with aortic regurgitation and left ventricular dysfunction: a change in the measuring stick. *J Am Coll Cardiol.* 1987;10:991-7.
19. Carabello BA, Williams H, Gashi AK, Kent R, Belber D, Maurer A, et al. Hemodynamic predictors of outcome in patients undergoing valve replacement. *Circulation.* 1986;74:1309-16.
20. Dickstein M, Spotnitz HM, Rose EA, Burkhoff D. Heart reduction surgery. An analysis of the impact on cardiac function. *J Thorac Cardiovasc Surg.* 1997;113:1032-40.
21. McCarthy PM, Takagaki M, Ochiai Y, Young JB, Tabata T, Shiota T, et al. Device-based change in left ventricular shape: a new concept for the treatment of dilated cardiomyopathy. *J Thorac Cardiovasc Surg.* 2001;122:482-90.
22. Hetzer R, Muller J, Weng Y, Wallukat G, Spiegelsberger S, Loebe M. Cardiac recovery in dilated cardiomyopathy by unloading with a left ventricular assist device. *Ann Thorac Surg.* 1999;68:742-9.
23. Maughan WL, Sunagawa K, Burkhoff D, Graves WL Jr, Hunter WC, Sagawa K. Effect of heart rate on the canine end-systolic pressure-volume relationship. *Circulation.* 1985;72:654-9.
24. Burkhoff D, Sugiura S, Yue DT, Sagawa K. Contractility-dependent curvilinearity of end-systolic pressure-volume relations. *Am J Physiol.* 1987;252:H1218-25.

ACD

Total Aortic Arch Replacement Through the L-Incision Approach

Ryuji Tominaga, MD, Kazuhiro Kurisu, MD, Yoshie Ochiai, MD, Atsuhiro Nakashima, MD, Munetaka Masuda, MD, Shigeki Morita, MD, and Hisataka Yasui, MD

Department of Cardiovascular Surgery, Kyushu University, Faculty of Medicine, Fukuoka, Japan

Background. Even though the median sternotomy is the standard approach for surgery involving the aortic arch, access to the site of distal anastomosis is problematic when the aortic pathology involves the distal arch. We recently developed an "L-incision" approach (a combination of a left anterior thoracotomy and upper half median sternotomy) for total arch replacement.

Methods. We reviewed our surgical technique and operative results for 11 patients who underwent total aortic arch replacement through the L-incision between July 1999 and July 2000. With a patient in a left anterolateral position, a left anterior thoracotomy was performed through the fourth to sixth intercostal space. An upper half median sternotomy followed. Operative exposure was enhanced with spring retractors. The proximal anastomosis (between the four branched graft and ascending aorta) was accomplished first. Upon completion of the proximal anastomosis, the heart was reperfused from one branch of the graft. The three arch vessels were subsequently reconstructed under deep hypothermia and retrograde cerebral perfusion. Antegrade cerebral perfusion was accomplished through the graft as the distal anastomosis (between the graft and descending thoracic aorta) was performed.

Results. No early operative deaths were observed. One patient sustained a permanent neurologic deficit. A transient recurrent laryngeal nerve palsy lasting 1 month occurred in 1 patient. No patient required reoperations for bleeding, nor did any patient develop a postoperative phrenic nerve palsy, aspiration pneumonia, or renal dysfunction.

Conclusions. The L-incision allows extensive replacement of the aortic arch and is associated with a low incidence of postoperative bleeding and respiratory insufficiency.

(Ann Thorac Surg 2003;75:121–5)

Among reported surgical approaches [1, 2], the median sternotomy is most frequently used for treatment of aortic arch aneurysms [3, 4]. However, in patients who present with an arch aneurysm, the exposure afforded by a median sternotomy is less than ideal. Inadequate visualization of the proximal descending thoracic aorta and phrenic and recurrent laryngeal nerves may result in distal anastomotic bleeding or postoperative nerve palsy. The combination of a full median sternotomy and left thoracotomy has been used frequently for total arch replacement. This extensive incision provides excellent operative exposure; however, the postoperative morbidity is considered excessive. Recently we used a hemi-clamshell incision ("L-incision" approach) [5] for total aortic arch replacement, particularly when the presence of a distal arch aneurysm demands better exposure of the distal anastomosis. We herein review our surgical technique and early postoperative results when replacing the aortic arch through the L-incision approach.

Accepted for publication Aug 12, 2002.

Address reprint requests to Dr Tominaga, Department of Cardiovascular Surgery, Kitakyushu Municipal Medical Center, 2-1-1, Bashaku, Kokurakitaku, Kitakyushu 802-0077, Japan; e-mail: tominaga21@fk.enjoy.ne.jp.

Published by Elsevier Science Inc

0003-4975/03/$30.00
PII S0003-4975(02)04300-X

Material and Methods

Patients

Between July 1999 and July 2000, we performed total aortic arch replacement through the L-incision approach, using the "proximal-first" technique [6], in 11 patients (Table 1). All patients were men aged 55 to 80 years (mean age, 68 years). Emergent operations were performed in 2 patients: 1 for rupture of an aortic arch aneurysm, and 1 for an ascending aortic dissection. The patient with vascular Behçet disease had previously undergone patch plasty of the aortic arch on two occasions: the first by a median sternotomy, the second by a left thoracotomy. Concomitant procedures included replacement of the entire descending thoracic aorta in 2 patients, coronary artery bypass grafting with saphenous vein grafts to the left anterior descending and the left circumflex arteries in 2 patients, and aortic valve resuspension in 1 patient. We were unable to cross-clamp the ascending aorta in 6 patients as intraoperative epiaortic echocardiography revealed severe atherosclerotic plaque.

Operative Techniques

All patients were intubated with a double-lumen endotracheal tube as the distal anastomosis was performed under single-lung anesthesia. With the patient in a left

Ann Thorac Surg
2003;75:121–5

Table 1. Patient Demographics

Patient No.	Age (y)	Etiology	Previous Operation	Concomitant Procedure
1	78	Arteriosclerosis		
2	70	Arteriosclerosis	AAA	
3	66	Combined		DAR
4	77	Arteriosclerosis		
5	61	Arteriosclerosis	AAA, amputation of legs	
6	59	Dissection (I)		AoV resuspension
7	53	Dissection (IIIb)		DAR
8	80	Arteriosclerosis		CABG
9	74	Arteriosclerosis	AAA	
10	74	Arteriosclerosis	AAA	CABG
11	55	Behçet disease	Patch plasty of Ao. arch	

AAA = resection of abdominal aortic aneurysm; Ao. arch = aortic arch; AoV = aortic valve; CABG = coronary artery bypass grafting; DAR = replacement of the entire descending thoracic aorta.

anterolateral position, a left fourth to sixth intercostal space (ICS) anterior thoracotomy was performed. An upper half median sternotomy followed (Fig 1). The left anterior thoracotomy was performed through the fourth ICS in 2 patients, the level being determined by the concomitant procedures. The left internal thoracic artery (LITA) was ligated and divided. Two spring retractors (Kent-boomerang/spring retractor, Takasago, Tokyo, Japan) were used; one to retract the left hemi-sternum in a left cranial direction and the other to retract the right hemi-sternum in a right caudal direction (Fig 2).

Fig 1. The L-incision for total arch replacement on the 14th postoperative day. The right axillary artery was used for arterial perfusion in this particular case.

In most instances, systemic arterial perfusion was performed through a cannula inserted into the ascending aorta. However, when intraoperative epiaortic echocardiography revealed atheromatous plaque in the ascend-

Fig 2. The operative view during total arch replacement with the L-incision through the fifth intercostal thoracotomy. Two spring retractors (SR) provided operative exposure. One retractor was used to retract the left hemi-sternum in a left cranial direction, while the second retractor withdraws the right hemi-sternum in the right caudal direction. This approach offers excellent access to both the ascending and descending thoracic aorta. The arch vessels (arch V) are also easily visualized. The aneurysm (AN) was located at the distal arch. (Ao = ascending aorta.)

ing aorta, arterial perfusion was performed through an 8-mm Hemashield graft (Hemashield Gold, Meadox Medicals, Inc, Oakland, NJ) that was anastomosed in an end-to-side fashion to the right axillary artery. Either the right or left femoral artery was exposed, and a 10-mm Hemashield graft anastomosed to it for lower body perfusion during arch vessel reconstruction. The arch vessels were never perfused through the femoral artery as retrograde aortic perfusion is associated with the risk of cerebral embolism. Two venous cannulas were inserted directly into the superior vena cava and inferior vena cava. Cardiopulmonary bypass (CPB) was established. A left ventricular vent was inserted through the left superior pulmonary vein, roof of the left atrium, or the left atrial appendage. Of these, the left superior pulmonary vein was preferred. Systemic cooling was initiated as the ascending aorta, aortic arch, and descending thoracic aorta were exposed. The fat pad containing the vagus and phrenic nerves was isolated by a tape.

The operative procedure is shown in Figure 3. The patient is cooled on CPB. An aortic cross-clamping is applied and antegrade cardioplegia administered. If mural disease precludes the application of an aortic cross-clamp, the aorta is transected under circulatory arrest and cardioplegia administered directly into the coronary ostia. The ascending aorta is anastomosed to a sealed graft with four branches (Hemashield Gold, Meadox Medicals, Inc, Oakland, NJ) (Fig 3A). Upon completion of the proximal anastomosis, the heart is reperfused through one branch of the Hemashield graft (Fig 3B). After confirming the rectal temperature is below 20°C, retrograde cerebral perfusion (RCP) is initiated. Retrograde cerebral perfusion was performed through the superior vena cava cannula, while maintaining the jugular vein pressure of 15 to 25 mm Hg with a flow rate of 300 to 400 mL/min. Lower body systemic perfusion protects the viscera and spinal cord, and is accomplished through the femoral artery after a cross-clamp is applied to the descending thoracic aorta. Reconstruction of three arch vessels (each branch of the graft to the left subclavian artery, left carotid artery, and innominate artery) is subsequently performed (Fig 3B). When arch vessels reconstruction is complete, RCP is discontinued and antegrade cerebral flow through the graft and arch vessels is restored (Fig 3C). The left lung is deflated to expose the descending thoracic aorta. The operating table is rotated 30 degrees from supine toward the patient's right side, and the surgeon moves from the patient's right to left side. Lower body systemic perfusion is discontinued and an open distal anastomosis (20- or 22-mm straight Hemashield graft-to-distal descending thoracic aorta) is performed using a modified elephant trunk technique (Fig 3D). While the open distal anastomosis is performed, the rectal temperature is kept below 20°C to protect the spinal cord. The arch graft is passed beneath the pedicle containing the vagus and phrenic nerves. The graft-to-graft anastomosis (four-branched graft to descending thoracic aorta) completes the operation (Fig 3E). As the graft-to-graft anastomosis is performed, femoral arterial perfusion is reestablished to remove air and debris. Upon completion of the distal anastomosis, the patient is rewarmed. We have reported this proximal-first technique previously in detail, using the four-branched graft (Hemashield; 26 or 28 mm with four branches (10, 10, 8, 8 mm) [6].

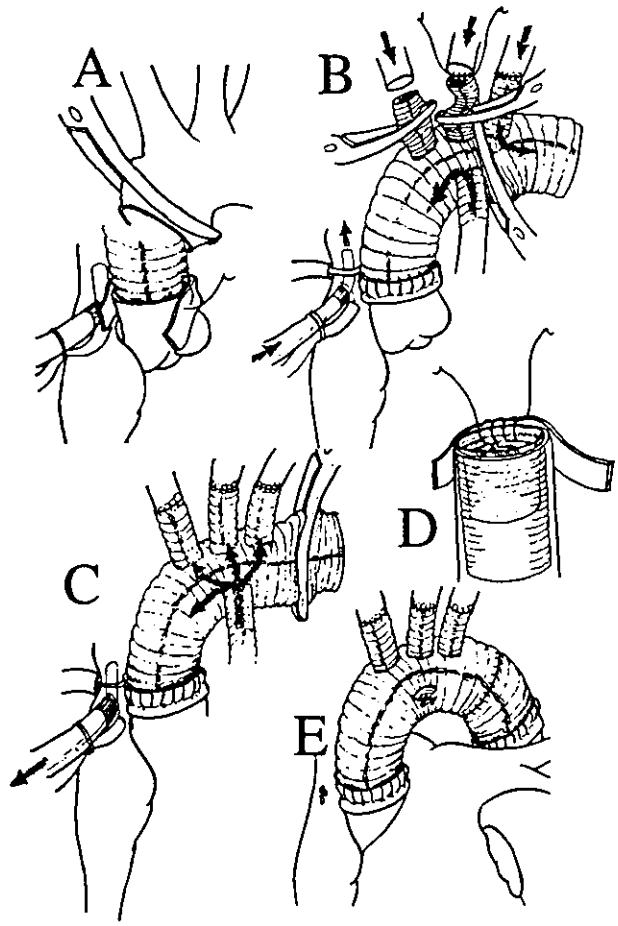

Fig 3. The "proximal first" operative technique for total arch replacement using a sealed graft with four branches. The first step is the anastomosis between the ascending aorta and the graft (A), followed by immediate restoration of myocardial reperfusion through one of four branches (B). The arch vessels are reconstructed under deep hypothermia and retrograde cerebral perfusion (B). After arch vessel reconstruction, antegrade cerebral blood perfusion is restored (C). The open distal anastomosis is accomplished using a modified elephant trunk technique (D). The final step is the anastomosis between the proximal and distal graft (E).

Results

The operative and CPB times ranged from 465 to 770 minutes and 182 to 334 minutes, respectively (Table 2). The aortic cross-clamp (myocardial ischemic time) and RCP times ranged from 15 to 64 minutes and 20 to 49 minutes, respectively. These times were determined, in part, by the need for concomitant procedures and the feasibility of aortic cross-clamping. The distal anastomosis (graft-to-descending thoracic aorta) was performed

Ann Thorac Surg
2003;75:121–5

Table 2. Perfusion Data and Outcome

Patient No.	Operation Time (min)	CPB Time (min)	AoX Time (min)	RCP Time (min)	LCA Time (min)	Complication	Outcome
1	485	194	17	39	35	None	Alive
2	510	182	25	40	37	None	Alive
3	680	215	20	39	30	None	Alive
4	535	222	19	37	23	None	Alive
5	465	202	19	20	26	Diffuse cerebral damage	Late death
6	590	324	64	36	47	None	Alive
7	770	334	28	27	27	Temporal general weakness	Alive
8	621	270	22	38	31	None	Alive
9	585	226	23	49	17	Recurrent laryngeal nerve palsy	Alive
10	660	214	15	33	72	None	Alive
11	540	193	32	36	30	None	Alive
Median	585	215	22	37	30		

AoX = ascending aortic cross-clamping; CPB = cardiopulmonary bypass; LCA time = lower body circulatory arrest time during open distal anastomosis; RCP = retrograde cerebral perfusion.

under lower body circulatory arrest with times ranging from 17 to 72 minutes. High-dose catecholamine administration was required in 1 patient to correct abnormal systemic vasodilation. No patients required a reoperation for bleeding or developed postoperative renal dysfunction.

The duration of postoperative mechanical ventilation ranged from 13 to 136 hours (mean 84 hours). The intensive care unit (ICU) length of stay ranged from 1.7 to 6.7 days (mean 5.5 days). These data excluded 2 patients who had neurologic complications. Long-term (longer than 72 hours) respiratory support was required in 4 patients. There were no early operative deaths. One patient developed hoarseness secondary to a recurrent laryngeal nerve palsy. However, the hoarseness resolved within 1 month of surgery. Phrenic nerve function was preserved in all patients. No patient developed aspiration pneumonia after the operation. One patient complained of intercostal wound pain and required intramuscular pentazocine for 1 week after the operation. Two patients developed postoperative neurologic deficits, although both patients had normal brain computed tomography; 1 patient had diffuse cerebral damage and the other patient had temporal general weakness. The patient with general weakness improved dramatically within 1 month of the operation. The patient with diffuse cerebral damage was transferred to a rehabilitation hospital and died of pneumonia 9 months after the operation. The remaining 10 patients were discharged from the hospital. All 10 patients are alive and well 9 to 21 months after the operation (mean follow-up 12 months).

Comment

The L-incision approach is, for a number of reasons, ideally suited for total aortic arch replacement particularly when aortic pathology involves the distal arch. First, the descending aorta is well visualized through the left anterior thoracotomy. Enhanced exposure facilitates performance of the distal anastomosis, thereby reducing the incidence of postoperative hemorrhage from that site. This anastomosis can also be performed more distally on the descending thoracic aorta. Second, both the phrenic and recurrent laryngeal nerves are easily isolated and preserved. These nerves play important roles in maintaining lung function, as a postoperative recurrent laryngeal nerve palsy can predispose patients, particularly the elderly, to aspiration pneumonia. Third, the lower part of the sternum is not divided. As thoracic integrity is maintained, pulmonary function is optimized and physical rehabilitation is enhanced. Fourth, improved visualization of the three arch vessels, especially the left subclavian artery, facilitates the anastomoses, thereby reducing RCP time. Finally, the L-incision approach always permits the ascending aorta to serve as the arterial cannulation site. Antegrade systemic perfusion reduces the incidence of neurologic complications particularly when atheromatous aneurysms involve the aortic arch [7, 8].

As the L-incision provides ready to access to both the ascending and descending aorta, it is well suited for extended replacement of the descending thoracic aorta. In 2 patients (#3, #7), we successfully replaced the entire thoracic aorta through this incision with a sixth ICS thoracotomy. In patient #7, we were able to reconstruct five intercostal arteries between T9 and T11 using short 10-mm diameter side grafts. As each intercostal artery required an individual side graft, the distal anastomosis took 72 minutes to complete. Consideration should be given to an additional thoracoabdominal incision when more complex intercostal arterial reconstruction is required. The L-incision approach may also be used in patients with a DeBakey type I aortic dissection in whom the entry site is unknown. If the entry point is thought to be in the descending thoracic aorta, with retrograde dissection across the arch [9], the L-incision allows ready identification of the entry point and facilitates performance of the distal anastomosis.

Disadvantages of the L-incision include sacrifice of the LITA and wound pain. In our series, the LITA was divided in all 11 patients; however, we believe that it can

be harvested and used as a conduit for concomitant coronary artery bypass grafting. Through the L-incision approach it would be feasible to perform coronary revascularization to either the left anterior descending coronary artery or the region of the left circumflex coronary artery. Inadequate exposure may make right coronary artery bypass difficult. One of 11 patients complained of intolerable wound pain. The patient had undergone a previous aortic operation and had received chronic steroid therapy. At his operation, osteoporosis resulted in multiple rib fractures that led to intolerable postoperative wound pain. A reduction in wound pain decreases the incidence of respiratory complications and facilitates patient rehabilitation and hospital discharge. Spring retractors provide excellent operative exposure and help prevent rib fractures.

We have used the proximal-first technique [6] for total arch replacement since 1995. Our goal in using this technique is to reduce myocardial ischemic and RCP time. In the current series the myocardial ischemic time (median 22 minutes) and RCP time (median 37 minutes) were shorter than those reported in a previous series [8]. With respect to cerebral injury, only 1 of 11 patients developed a permanent neurologic deficit. This patient had undergone a prior abdominal aortic aneurysmectomy and bilateral leg amputation due to arteriosclerosis obliterans. Mural atheroma, which may not be detected by epiaortic echocardiography, may shower the central circulation, resulting in diffuse cerebral damage.

In our small series, 4 of 11 (36%) patients required long-term (longer than 72 hours) respiratory support. However, respiratory insufficiency did not result in patient death. Ergin and associates [10] reported that 27% of patients (54 of 200 patients) who underwent thoracic aortic aneurysmectomy using a median sternotomy experienced postoperative respiratory insufficiency. The incidence of respiratory insufficiency in Ergin's series and the current series is similar. It may be possible to reduce the incidence of postoperative pulmonary dysfunction by gentle manipulation of the left lung during the operation. With respect to the ICU length of stay, Hoefer and colleagues [11] reported a median postoperative ICU stay of 5 days (range 1 to 72 days) after surgery for acute aortic dissection, a result that is similar to the current series.

In conclusion, the L-incision approach for total arch replacement facilitates extensive replacement of the thoracic aorta while reducing the potential for postoperative bleeding and respiratory complications. Our favorable initial experience justifies further clinical evaluation of this technique.

We gratefully thank Dr Wayne Richenbacher for his editorial assistance.

References

1. Sasaguri S, Yamamoto S, Fukuda T, Hosoda Y. Retrograde cerebral perfusion through antero-axillary thoracotomy in the aortic arch surgery. Eur J Cardiothorac Surg 1997;11:657–60.
2. Imazeki T, Yamada T, Irie Y, Katayama Y, Kiyama H. Trapdoor thoracotomy as a surgical approach for aortic arch aneurysm. Ann Thorac Surg 1998;66:272–4.
3. Borst HG, Heinemann MK, Stone CD. Surgical treatment of aortic dissection. New York: Churchill Livingstone, 1996.
4. Svenson LG, Crawford ES. Cardiovascular and vascular disease of the aorta. Philadelphia: WB Saunders, 1997.
5. Bains MS, Ginsberg RJ, Jones WG Jr, et al. The clamshell incision: an improved approach to bilateral pulmonary and mediastinal tumor. Ann Thorac Surg 1994;58:30–2.
6. Tominaga R, Kurisu K, Ochiai Y, et al. Early proximal aortic reperfusion in total arch replacement. Jpn J Vasc Surg 2002;11:511–6.
7. Westaby S, Katsumata T. Proximal aortic perfusion for complex arch and descending aortic disease. J Thorac Cardiovasc Surg 1998;115:162–7.
8. Rokkas CK, Kouchoukos NT. Single-stage extensive replacement of the thoracic aorta: the arch-first technique. J Thorac Cardiovasc Surg 1999;117:99–105.
9. von Segesser LK, Killer I, Ziswiler M, et al. Dissection of the descending thoracic aorta extending into the ascending aorta. A therapeutic challenge. J Thorac Cardiovasc Surg 1994;108:755–61.
10. Ergin MA, Galla JD, Lansman SL, Quintana C, Bodian C, Griepp RB. Hypothermic circulatory arrest in operations on the thoracic aorta: determinants of operative mortality and neurologic outcome. J Thorac Cardiovasc Surg 1994;107:788–99.
11. Hoefer D, Ruttman E, Riha M, et al. Factors influencing intensive care unit length of stay after surgery for acute aortic dissection type A. Ann Thorac Surg 2002;73:714–8.

Transfection With a Dominant-Negative Inhibitor of Monocyte Chemoattractant Protein-1 Gene Improves Cardiac Function After 6 Hours of Cold Preservation

Noriyoshi Kajihara, MD; Shigeki Morita, MD; Takahiro Nishida, MD; Hideki Tatewaki, MD; Masataka Eto, MD; Kensuke Egashira, MD; Hisataka Yasui, MD

Background—Monocyte chemoattractant protein-1 (MCP-1), a potent chemotactic factor for monocytes, is induced during ischemia-reperfusion. As monocytes might play an important causative role in reperfusion injury, we investigated if inhibition of monocyte activation could attenuate ischemia-reperfusion injury and thereby improve cardiac preservation. To inhibit monocyte activation, we transfected a dominant-negative inhibitor of MCP-1 (7ND) gene in an animal model.

Methods and Results—We used an isolated rabbit heart preparation perfused with support-rabbit blood and transfected 7ND genes to skeletal muscle of the support rabbits (n=7) using electroporation technique; causing an elevation of serum 7ND level to 20±7 pg/mL at 5 days after transfection. Animals receiving empty plasmid served as controls (n=7). Five days after transfection, hearts from other rabbits were excised, stored in UW solution for 6hours, and perfused with blood from transfected support rabbits. The 7ND group showed better cardiac output (128.7±17.9 versus 81.6±19.8 mL/min; $P<0.01$), lower serum CK-MB levels (5.0±1.8 versus 11.1±2.9 ng/mL; $P<0.01$), lower serum IL-1β levels (257.2±23.2 versus 311.2±37.4pg/mL; $P<0.05$), and lower serum TNF-α levels (19.0±8.4 versus 35.1±13.0pg/mL; $P<0.05$). The numbers of infiltrating cells in myocardium were significantly reduced in the 7ND group.

Conclusions—Inhibition of MCP-1 with 7ND gene transfection reduced cytokine activation, attenuated myocardial damage, and improved cardiac function after 6 hours of preservation. These results show that MCP-1 plays an important role in ischemia-reperfusion injury. (***Circulation.*** **2003;108[suppl II]:II-213-II-218.)**

Key Words: gene therapy ■ leukocytes ■ reperfusion injury ■ cytokines

Myocardial ischemia-reperfusion injury is believed to be associated with inflammatory reactions involving various types of cells and cytokines.[1-3] Leukocytes are recognized as a major factor in ischemia-reperfusion injury. A number of studies, most focusing on neutrophils, have demonstrated harmful effects of leukocytes, such as the production of cytokines and oxygen radicals, adhesion to endothelium, and activation of complement systems.

Recently, in addition to neutrophils, several studies have demonstrated that in the early phase of reperfusion monocyte chemoattractant protein-1 (MCP-1) is induced and monocytes migrate into the reperfused myocardium.[4-6] We thus hypothesized that inhibition of monocyte activation would attenuate ischemia-reperfusion injury.

To inhibit monocyte activation we used a 7ND skeletal muscle transfection model.[7-11] 7ND is an N-terminal deletion mutant of the MCP-1 gene and has been shown to be a dominant negative inhibitor of MCP-1.[12,13] Studies show that 7ND protein is secreted from transfected skeletal muscle cells into circulating blood, and subsequently blocks MCP-1-induced chemotaxis in remote organs.[7-11]

Using a blood perfused isolated rabbit heart preparation,[14,15] we investigated whether the inhibition of monocyte activation with 7ND gene transfer could attenuate ischemia-reperfusion injury.

Methods

Experimental Animals

Japanese white rabbits (KBT oriental, Tokyo, Japan) weighing from 2.9 to 3.3 kg were used (27 for preliminary experiments, and 14 each as heart donors, support rabbits, and blood donors). This experiment was reviewed by the Committee on the Ethics of Animal Experiments of the Faculty of Medicine, Kyushu University, and was carried out under the Guidelines for Animal Experiments of the Faculty of Medicine, Kyushu University, and the Law (No. 105) and Notification (No.6) of the Japanese Government.

From the Department of Cardiovascular Surgery, and Department of Cardiovascular Medicine, Graduate School of Medical Sciences, Kyushu University, Fukuoka, Japan.

Correspondence to Shigeki Morita, MD, Department of Cardiovascular Surgery, Graduate School of Medical Sciences, Kyushu University, 3-1-1 Maidashi, Higashi-ku, Fukuoka, 812-8582, Japan. Phone: 81-92-642-5557; Fax: 81-92-642-5566; E-mail: morita@heart.med.kyushu-u.ac.jp.

Circulation is available at http://www.circulationaha.org

DOI: 10.1161/01.cir.0000087426.18858.3a

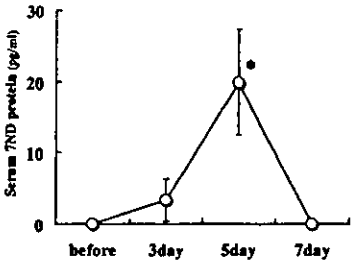

Figure 1. Line graph shows the levels of 7ND protein in serum after 7ND gene transfection. Levels significantly increase at 5day. *$P<0.01$ versus before. All values are mean±SD (n=5).

Expression Vector Mutant

Human 7ND cDNA was constructed by recombinant polymerase chain reaction using a wild-type MCP-1 cDNA as template and cloned into the *Bam* HI (5′) and *Not* I (3′) site of the pcDNA3 expression vector plasmid.

Gene Transfer

Rabbits received intramuscular injections of empty plasmid or pcDNA3–7ND plasmid DNA (500 μg/kg) into the femoral muscle. Transgene expression was enhanced by intramuscular electroporation at the injection site immediately after injection. Six electronic pulses of 50V, 100 ms were applied to each injection site using an electric pulse generator (CUY201; BEX, Tokyo, Japan).

To determine the optimal timing for the experiment of ischemia-reperfusion, we performed preliminary experiments to examine at what day the 7ND protein level peaked after 7ND injection. We measured serum 7ND protein levels before, 3, 5, and 7 days after gene transfection by enzyme linked immunoassay using human MCP-1 ELISA kit (BioSource International, Inc, Camarillo, CA). Because this human MCP-1 ELISA kit does not react with the rabbit MCP-1, it was considered that serum 7ND protein levels could be measured by the use of this human ELISA kit. The serum 7ND protein levels peaked at 5 days after 7ND gene transfection (20±7 pg/mL) (Figure 1). The rabbits injected with empty plasmid showed no detectable 7ND protein in the serum.

To confirm the effect of 7ND, recombinant human MCP-1 (2 μg/100 μmL) or PBS (100 μmL) was injected into the dermis 5 days after gene transfer to confirm the effect of 7ND. Twenty-four hours after the intradermal injection of MCP-1, a marked infiltration of mononuclear cells was detected in the MCP-1 injected site of rabbits that received injections of empty plasmid (Figure 2A). On the other hand, few infiltrated mononuclear cells were detected in the MCP-1 injected site of rabbits that received injections of 7ND genes (Figure 2B). At the PBS injected skin sites, no infiltration cells were detected (Figure 2C). Based on the data gained from these experiments, we decided to perform the main ischemia-reperfusion experiments 5 days after transfection of support rabbits with 7ND.

Donor Heart Management

The rabbits were anesthetized using sodium thiamylal (20 mg/kg) and intubated with a tracheal tube connected to a mechanical ventilator (model SN-480 to 5, Shimano, Tokyo, Japan) utilizing 100% oxygen. For further anesthesia, vecuronium bromide (1 mg/kg) and fentanyl citrate (700 μg/kg) were given. After performing a median sternotomy, the thymus and the pericardium were carefully removed and then the heart and aortic arch exposed. After heparinization (1500 U/kg), the innominate artery was cannulated to administer University of Wisconsin (UW) solution (ViaSpan, Netherlands Production Laboratory for Blood Transfusion Apparatus and Infusion Fluids, Inc, Emmer-Compascuum, Netherlands). After the inferior vena cava was transected to decompress the heart, the aortic arch was cross-clamped and UW solution (0°C, 20 mL/kg) was infused at constant flow rate of 12 mL/min with a syringe infusion pump (Compact Infusion Pump Model 975, Harvard Apparatus, South Natick, MA). The hearts were quickly excised and immersed

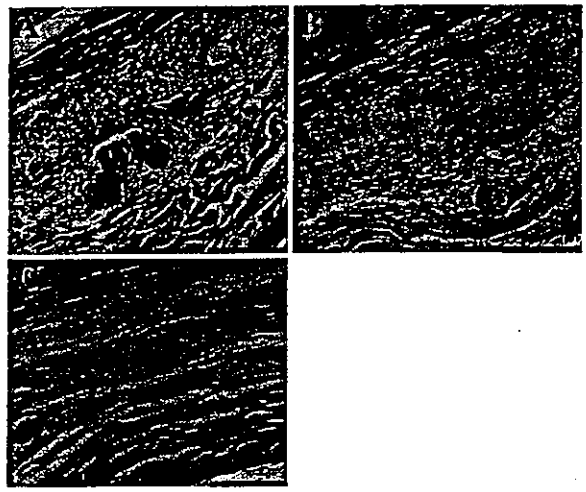

Figure 2. HE staining of MCP-1 or PBS injected skin sites 24 hours after injection. Bar=200 μm. (A) In recombinant human MCP-1 injected skin sites of the rabbit that was transfected the empty plasmid, a marked infiltration of mononuclear cells is detected. (B) In recombinant human MCP-1 injected skin sites of the rabbit that was transfected with 7ND genes, a few infiltrated mononuclear cells are detected. (C) In PBS-injected skin sites, no infiltration cells are detected.

in cold UW solution (0°C) during preservation. The temperature was maintained by a heat-exchanger (model RTE-210, Neslab instruments, Inc, Newington, NH).

Support Rabbit and Cross-Circulation System

The support rabbits were anesthetized and pretreated in the same manner as the donor rabbits. Anesthesia was maintained with constant infusion of fentanyl citrate (200 μg/h) and vecuronium bromide (1 mg/h). After heparinization (1500 U/kg), the common carotid artery and the external jugular vein were exposed and cannulated. Oxygenated blood from the common carotid artery of the support rabbit was introduced by a microtube pump (model MP-3, Tokyo Rikakikai Inc, Tokyo, Japan) to a cannula connected to the ascending aorta of the donor heart. The blood draining from the system was then returned to the jugular vein by another microtube pump (Figure 3A). During use of this system, hematocrit of perfusion blood was maintained at 23% by the using blood donor rabbits. Arterial blood gas analyses of the support rabbit were done with a pH/blood gas analyzer (model IL-1304, Instrumentation Laboratory, Barcelona, Spain). The femoral artery pressure of the support rabbit was also continuously monitored.

Measurement of Left Ventricular Function in Working Model

We measured LV function after 6-hours of preservation using a working preparation, as previously described.[14] The donor heart was perfused through the aorta and then Langendorff preparation perfusion was initiated (Figure 3A). Perfusion pressure was maintained at 60mmHg and blood temperature maintained at 37°C. The superior and inferior vena cava and pulmonary veins were closed, and a double lumen cannula was inserted into the left atrium. One lumen of the double lumen cannula was connected to a pressure transducer to measure left atrial pressure (LAP), and the other to an atrial reservoir. Aortic flow rate was measured by an in-line electromagnetic flow probe (model 2N764, Transonic System Inc, NY) connected to a flowmeter (model T206, Transonic System Inc). Aortic pressure was measured from a sidearm in the aortic tract (Figure 3B). All signals (pressures and flows) were continuously monitored on an oscillograph (polygraph 360 system, NEC Sanei, Tokyo, Japan), digitized on-line at 200Hz with an analog-to-digital converter (MacLab System, AD Instruments, Ltd, Dunedin North, New Zea-

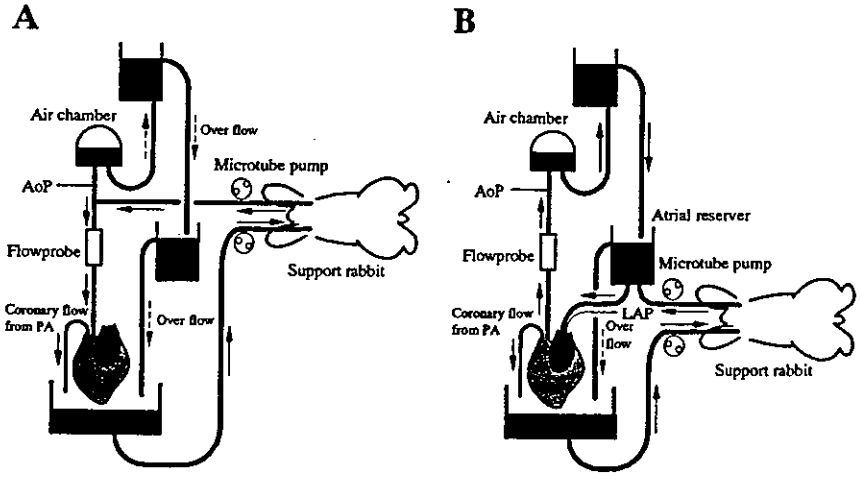

Figure 3. Cross-circulated rabbit heart preparation. (A) In the Langendorff preparation, oxygenated blood from the common carotid artery of the support rabbit was introduced to an aortic inflow tract of this system. The coronary venous blood was collected and returned to the support rabbit. (B) In the working preparation, the left atrium was cannulated with a double lumen cannula. The blood collected in the atrial reservoir was ejected by the heart. AoP=aortic pressure, PA=pulmonary artery, LA=left atrium, LAP=left atrial pressure.

land) and recorded on a digital computer (PowerBook 550C, Apple Computer, Inc, Cupertino, CA).

In the working preparations, hearts were paced atrially at 250 beat/min and aortic afterload pressure fixed at 60 mm Hg. Aortic flow rates were measured at points of varied LAP. Systolic and diastolic pressures, the variables determined by the cardiac output and the stiffness or compliance of the afterload system, varied according to increases in LAP; whereas mean pressure was kept stable (60 mm Hg) throughout the measurements. Based on these data, we determined the Frank-Starling curve.

Experimental Protocol

The rabbits were divided into two groups according to the transfection of 7ND genes. The 7ND group (n=7) was transfected with pcDNA3-7ND plasmid DNA (500 μg/kg) and the control group (n=7) was transfected with the empty plasmid. Support rabbits and blood donors were transfected into their femoral muscle.

Five days after transfection, the heart from another rabbit was excised and stored in UW solution for 6 hours. After the preservation period, the heart was perfused with blood from a transfected support rabbit with the Langendorff preparation at 60 mm Hg of perfusion pressure. We measured the serum creatine kinase MB (CK-MB), interleukin-1β (IL-1β), and tumor necrosis factor-α (TNF-α) levels in the coronary effluents at 10, 60, and 120 minutes after reperfusion. At 40 and 120 minutes after reperfusion, we measured left ventricle function in working preparation. The donor heart was paced atrially at 250 beat/min. After the measurement at 120 minutes after reperfusion, the donor heart was quickly removed from the cross-circulation system and the left ventricles were immersed in 10% paraformaldehyde histopathological examination. For a reference, we performed an experiment in which freshly harvested hearts without preservation were attached to the system using a nontransfected support rabbit (n=3). The support rabbit was killed with a lethal dose of anesthesia.

Measurement of CK-MB, IL-1β, and TNF-α

The serum CK-MB levels were measured by chemiluminescent immunoassay, and the IL-1β and TNF-α levels by enzyme linked immunoassay using a rat IL-1β and TNF-α ELISA kit (BioSource International, Inc).

Histopathology and Number of Infiltrating Cells in Myocardium

Cardiac tissue was fixed in 10% paraformaldehyde. Tissue was dehydrated, embedded in paraffin and cut into 5 μm thick slices, and then stained with Hematoxylin and Eosin. The number of infiltrating cells in myocardium was counted as the sum of the cell counts on 3 fields at ×400 magnification.[16]

Statistical Analysis

Results for each group are expressed as mean±SD. Values between the two groups were examined by two-way repeated measures

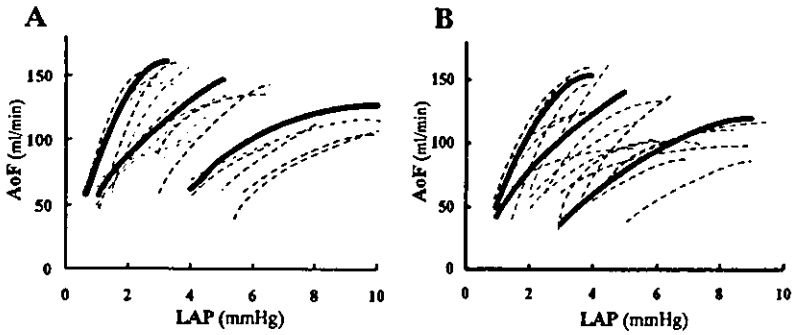

Figure 4. Frank-Starling curve data obtained in this study. The red thick line represents the fitted Frank-Starling curve in the 7ND group (n=7). The red dashed lines show the individual curves in the 7ND group. The blue thick line represents the fitted Frank-Starling curve in the control group (n=7). The blue dashed lines show the individual curves in the control group. The black thick line represents the fitted Frank-Starling curve of freshly harvested hearts without preservation and gene transfection (n=3). (A) Frank-Starling curve data obtained at 40 minutes after reperfusion. The curve was significantly shifted to the left side in the 7ND group ($y=-0.98x^2+28.82x+32.32$) compared with that in the control group ($y=-1.70x^2+35.11x-51.38$). For reference, we also show fitted curves of freshly harvested hearts without preservation and gene transfection ($y=-3.41x^2+55.41x+38.82$). (B) Frank-Starling curve data obtained at 120 minutes after reperfusion. The curve was significantly shifted to the left side in 7ND group ($y=-2.46x^2+37.08x+9.15$) compared with that in control group ($y=-2.30x^2+40.82x-67.88$). We show fitted curves of freshly harvested hearts ($y=-3.41x^2+55.41x+38.82$). AoF=aortic flow, LAP=left atrial pressure.

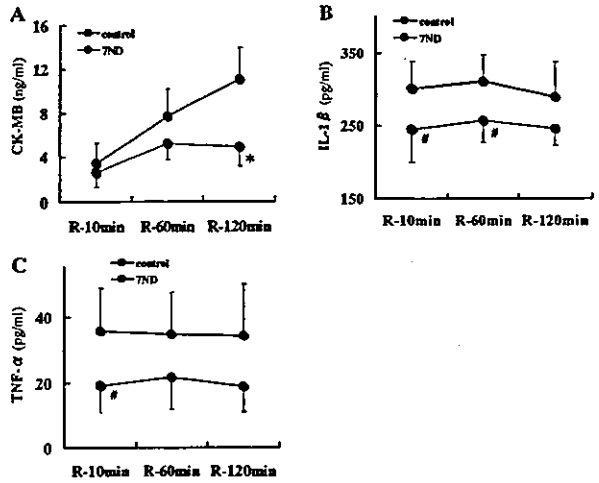

Figure 5. (A) Bar graph shows serum CK-MB levels. Serum CK-MB level in the 7ND group is significantly lower than that in the controls at 120 minutes after reperfusion. *$P<0.01$ versus control group. (B) Bar graph shows serum IL-1β levels. Serum IL-1β levels in the 7ND group are significantly lower than those in control group at 10 minutes and 60 minutes after reperfusion. #$P<0.05$ versus control group. (C) Bar graph shows serum TNF-α levels. In the 7ND group, serum TNF-α level is significantly lower than that in the controls at 10 minutes after reperfusion. #$P<0.05$ versus control group. All values are mean±SD.

analysis of variance (ANOVA). When ANOVA showed a significant intergroup difference, unpaired Student's t test was used to examine the difference in each parameter. The relationship between LAP and AoF was analyzed by a multiple regression model using a dummy variable technique to investigate intergroup difference.[17] Significance was designated as a probability value of less than 0.05

Results

Between the two groups no significant differences were observed in body weights of donor rabbits. During the experiments, hemodynamics of the support rabbits were stable and systolic blood pressure was maintained at over 100 mm Hg. Minimum alterations in the arterial carbon dioxide tension, pH, and arterial bicarbonate levels were observed in the support rabbits.

Cardiac Function: Frank-Starling Curves

At both 40 and 120 minutes after reperfusion, the fitted Frank-Starling curve obtained by a multiple linear regression model was significantly shifted to the left ($P<0.01$) in the 7ND group compared with that of the control group (Figure 4). We also show fitted curves of freshly harvested hearts without preservation and gene transfection in Figure 4.

Serum Levels of CK-MB, IL-1β, and TNF-α

Serum CK-MB levels in the 7ND group were significantly lower than those in the control group at 120 minutes after reperfusion (5.0±1.8 versus 11.1±2.9 ng/mL, $P<0.01$) (Figure 5A).

Serum IL-1β levels in the 7ND group were significantly lower than those in the control group at 10 minutes (244.7±46.2 versus 300.6±37.8 pg/mL, $P<0.05$) and 60 minutes after reperfusion (257.2±23.2 versus 311.2±37.4 pg/mL, $P<0.05$) (Figure 5B).

Serum TNF-α levels in the 7ND group were significantly lower than those in the control group at 10 minutes after reperfusion (35.1±13.1 versus 19.0±8.4 pg/mL, $P<0.05$) (Figure 5C).

Histopathology and Number of Infiltrating Cells in Cardiac Tissue

Histological appearances of myocardium from the 2 groups are shown in Figure 6. The extravasation of polymorphonuclear and mononuclear leukocytes was recognized in the myocardium from the control group (Figure 6A). On the other hand, few leukocytes existed in myocardium from the 7ND

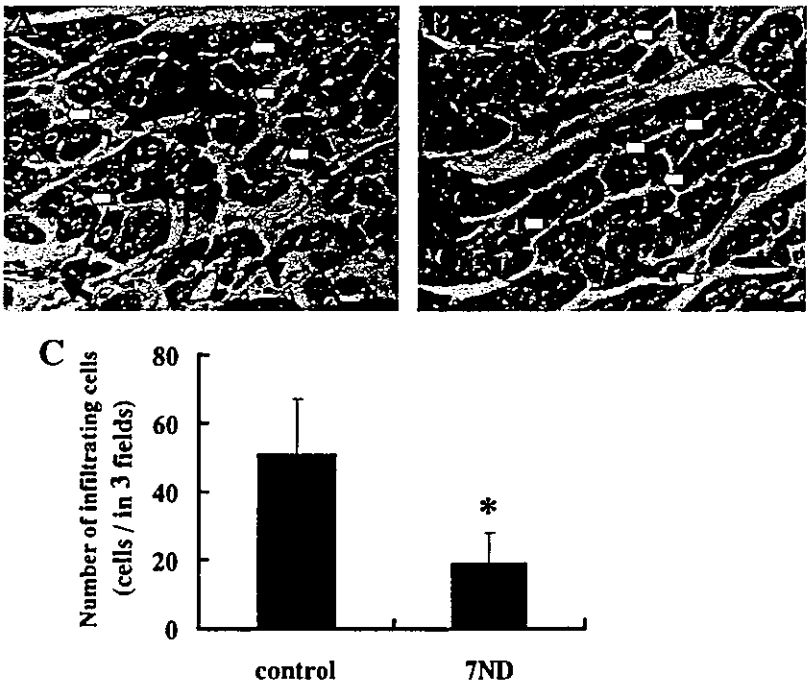

Figure 6. (A) HE staining of myocardium from the control group. Extravasation of polymorphonuclear and mononuclear infiltrating cells is recognized. (B) HE staining of myocardium from the 7ND group; few infiltrating cells exist. Closed arrow=infiltrating cell, Open arrow=endothelial cell, Bar=200 μm. (C) Bar graph shows the number of infiltrating cells in myocardium. The number of infiltrating cells is significantly reduced in the 7ND group compared with controls. The number is the sum of the cell counts on 3 fields at a ×400 magnification. *$P<0.01$ versus control group. All values are mean±SD.

group (Figure 6B). The number of infiltrating cells in myocardium was significantly reduced in the 7ND group compared with the control group (19.0±8.9 versus 51.0±16.0 cells / in 3 fields; $P<0.01$) (Figure 6C).

Discussion

In this study we demonstrated that inhibition of MCP-1 with 7ND gene transfection reduced cytokine activation, attenuated myocardial damage and improved cardiac function after 6 hours of cold preservation. Our results indicated that monocytes and their chemoattractant, MCP-1, played an important role in ischemia reperfusion.

MCP-1 is a member of a family of proinflammatory cytokines called chemokines, which are structurally related.[18] Chemokines affect the migration and activation of various types of leukocytes. MCP-1, a prototypic chemokine belonging to the C-C family, binds to MCP-1 receptor (CCR2) on monocytes as a dimmer and exhibits chemoattractant potential for monocytes, but not for neutrophils. It has been demonstrated that MCP-1 expression is increased in chronic inflammatory diseases such as atherosclerosis and rheumatic arthritis.[18] As has the migration of monocytes and inducement of MCP-1 at an early phase of reperfusion.[4-6] Kumar et al have reported that MCP-1 mRNA was induced in endothelium of the small veins in ischemic and reperfused canine myocardium.[6] Matsumori et al reported that plasma concentrations of MCP-1 are increased in patients after acute myocardial infarction.[5] These studies indicate that increased production of MCP-1 and subsequent monocyte infiltration are observed at the reperfusion phase of myocardial ischemia. In this study, we directly inhibited MCP-1 and prevented activation of monocytes in a myocardial ischemia and reperfusion model, and showed that inhibition of MCP-1 attenuated reperfusion injury and preserved post-ischemia cardiac function. Our finding of improved cardiac function with MCP-1 inhibition was in accordance with the study of Ono et al that showed the favorable effects of administrating anti-MCP-1 antibody to reduce the infarct size in a rat model of ischemia-reperfusion.[19]

Although the exact mechanism by which cardiac function is improved with inhibition of MCP-1 is not clear, it would be highly probable that reduced production of inflammatory cytokines with MCP-1 inhibition was the main factor attenuating ischemia reperfusion injury. Herskowitz et al[20] and Formigli et al[4] showed that monocytes are the main source of inflammatory cytokines in a myocardial ischemia-reperfusion model in rats and pigs, respectively. Inflammatory cytokines such as IL-1β and TNF-α were demonstrated to possess negative inotropic effects,[21,22] and these were also shown to have chemoattractant actions for neutrophils,[23,24] which play an important role in ischemia-reperfusion. In our study, the number of infiltrating cells in myocardium was significantly reduced in the 7ND group. Infiltrated cells found in the control group were polymorphonuclear and mononuclear leukocytes, which indicated that 7ND reduced the number of polymorphonuclear leukocytes as well. These findings suggested that inflammatory cytokines produced by monocytes activated neutrophils and further promoted inflammatory reactions in ischemia-reperfusion. Since 7ND and MCP-1 do not exhibit direct effects on neutrophils, it is highly probable that monocytes play a crucial role in the cascade of ischemia-reperfusion injury.

We used 7ND genes to perform anti-MCP-1 therapy in this study. 7ND lacks amino-terminal amino acids 2 to 8 in the amino sequence of MCP-1,[12,13] and forms a heterodimer with wild type MCP-1. This heterodimer has been shown to bind to CCR2 and to work as a dominant negative inhibitor of MCP-1.[13] 7ND protein is produced by 7ND gene transfection to skeletal muscle and intensively inhibits monocyte infiltration.[7-11] Although a logical strategy to inhibit MCP-1 would be to administer 7ND protein at the time of reperfusion, we used 7ND gene transfection to the skeletal muscle because 7ND protein was not available.

In this study, we used a mutant gene of human MCP-1 in a rabbit model. The amino acid sequence similarity of rabbit MCP-1 to human MCP-1 is high and it has been demonstrated that human MCP-1 has a high affinity for rabbit monocytes.[25] Indeed, we showed in the present study that 7ND gene transfer inhibited monocyte infiltration by intradermal injection of human MCP-1 in rabbits. Because recombinant rabbit MCP-1 was not available, we were not able to prove that 7ND gene transfer blocks activity of rabbit MCP-1. This is a limitation; however, we proved that inhibition of human MCP-1 induced monocyte infiltration into rabbit dermis by 7ND gene transfer. Since the sequence of human MCP-1 and rabbit MCP-1 show high similarity, it is highly probable that human 7ND may inhibit rabbit MCP-1. In fact, other studies show that 7ND is effective in experiments using mice, rats, and monkey.[7-11] We recently showed suppression of macrophage recruitment into injured rabbit carotid artery by 7ND gene transfer.[26] Considering those results, we believe it is safe to assume that 7ND blocked the action of rabbit MCP-1.

We used a blood-perfused isolated working rabbit heart model developed in our laboratory.[14,15] Compared with isolated heart preparations perfused with crystalloid solutions, our blood-perfused model is well suited to investigate the process of ischemia-reperfusion, which involves numerous cellular components such as leukocytes and platelets. A potential limitation of our preparation is that because it is in extra-corporeal circulation, which allows blood to contact foreign surfaces; running an extra-corporeal circulation per se might have activated inflammatory process. To investigate the influence of our cross-circulation system on inflammatory reactions, we performed preliminary experiments running extra-corporeal circulation with support rabbits attached but without connecting the donor heart to the preparation. These showed that there were no increases in serum cytokine levels or blood leukocyte counts. Thus, we assumed that the increases in IL-1β and TNF-α observed in the controls were the result of ischemia and reperfusion.

The drug delivery system used in this study is a limitation; currently, 7ND protein has not been manufactured, delaying further study on the clinical application of 7ND. We modeled our experiments for hypothermic storage, but further refinement is needed in 7ND administration for clinical application. One possibility is to manufacture 7ND protein and deliver it

intravenously; thus, 7ND may be administered to patients undergoing heart transplantation or open-heart surgery.

In conclusion, inhibition of MCP-1 with 7ND transfection reduced cytokine activation, attenuated myocardial damage and improved cardiac function after 6 hours of cold preservation. These results indicate that MCP-1 plays an important role in ischemia-reperfusion injury. 7ND gene transfection might become a useful strategy for attenuating ischemia-reperfusion injury.

Acknowledgments

This study was supported by grants-in-aid for scientific research (14571271, 14657172, 14207036) from the Ministry of Education, Science and Culture, Tokyo, Japan, by Health Science Research Grants (Comprehensive Research on Aging and Health, and Research on Translational Research) from the Ministry of Health Labor and Welfare, Tokyo, Japan, and by the Program for Promotion of Fundamental Studies in Health Sciences of the Organization for Pharmaceutical Safety and Research, Tokyo, Japan.

References

1. Entmann ML, Smith CW. Postreperfusion inflammation: a model for reaction to injury in cardiovascular disease. *Cardiovasc Res.* 1994;28: 1301–1311.
2. Weiss SJ. Tissue destruction by neutrophils. *N Engl J Med.* 1989;320: 365–376.
3. Chandrasekar B, Colston JT, Geimer J, et al. Induction of nuclearκB but notκB: responsive cytokine expression during myocardial reperfusion injury after neutropenia. *Free Rad Biol Med.* 2000;28:1579–1588.
4. Formigli L, Manneschi LI, Nediani C, et al. Are macrophages involved in early myocardial reperfusion injury? *Ann Thorac Surg.* 2001;71: 1596–1602.
5. Matsumori A, Furukawa Y, Hashimoto T, et al. Plasma level of the monocyte chemotactic and activating factor/monocyte chemoattractant protein-1 are elevated in patients with acute myocardial infarction. *J Mol Cell Cardiol.* 1997;29:419–423.
6. Kumar AG, Ballantyne CM, Michael LH, et al. Induction of monocyte chemoattractant protein-1 in the small veins of the ischemic and reperfused canine myocardium. *Circulation.* 1997;95:693–700.
7. Egashira K, Zhao QW, Kataoka C, et al. Importance of monocyte chemoattractant protein-1 pathway in neointimal hyperplasia after peri-arterial injury in mice and monkeys. 2002;90:1167–1172.
8. Egashira K, Koyanagi M, Kitamoto S, et al. Anti-monocyte chemoattractant protein-1 gene therapy inhibits vascular remodeling in rats: blockade of MCP-1 activity after intramuscular transfer of a mutant gene inhibits vascular remodeling induced by chronic blockade of NO synthesis. *FASEB J.* 2000;14:1974–1978.
9. Ni W, Egashira K, Kitamoto S, et al. New anti-monocyte chemoattractant protein-1 gene therapy attenuates atherosclerosis in apolipoprotein e-knockout mice. *Circulation.* 2001;103:2096–2101.
10. Inoue S, Egashira K, Ni W, et al. Anti-monocyte chemoattractant protein-1 gene therapy limits progression and destabilization of established atherosclerosis in apolipoprotein e-knockout mice. *Circulation.* 2002;106:2700–2706.
11. Usui M, Egashira K, Ohtani C, et al. Anti-monocyte chemoattractant protein-1 gene therapy inhibits restenotic changes (neointimal hyperplasia) after balloon injury in rats and monkeys. *FASEB.* 2002;16(5): 1838–1840.
12. Zhang YJ, Rutledge BJ, Rollins BJ. Structure/activity analysis of human monocyte chemoattractant protein-1(MCP-1) by mutagenesis. *J Biol Chem.* 1994;269:15918–15924.
13. Zhang YJ and Rollins BJ. A dominant negative inhibitor indicates that monocyte chemoattractant protein-1 functions as a dimmer. *Mol Cell Biol.* 1995;15:4851–4855.
14. Nishida T, Morita S, Miyamoto K, et al. The effect of lazaroid (U74500A), a novel inhibitor of lipid peroxidation, on 24-hour heart preservation: a study based on a working model using cross-circulated blood perfused rabbit hearts. *Transplantation.* 1996;61:194–199.
15. Nishida T, Morita S, Miyamoto K, et al. Lazaroid (U74500) prevents vascular and myocardial dysfunction after 24-hour heart preservation: a study based on cross-circulation blood-perfused rabbit hearts. *Circulation.* 1996;94 (suppl II):II326–II331.
16. Yamashiro S, Takeya M, Kuratsu J, et al. Intradermal injection of monocyte chemoattractant protein-1 induces emigration and differentiation of blood monocytes in rat skin. *Int Arch Allergy Immunol.* 1998; 115:15–23.
17. Glantz SA, Slinker BK. Primer of applied regression and analysis of variance. New York: McGraw-Hill; 1990.
18. Rollins BJ. Chemokines. *Blood.* 1997;90:909–928.
19. Ono K, Matsumori A, Furukawa Y, et al. Prevention of myocardial reperfusion injury in rats by an antibody against monocyte chemotactic and activating factor/monocyte chemoattractant protein-1. *Lab Invest.* 1999;79:195–203.
20. Herskowits A, Choi S, Ansari AA, et al. Cytokine mRNA expression in postischemic/ reperfused myocardium. *Am J Pathol.* 1995;146:419–428.
21. Yokoyama T, Vaca L, Rossen RD, et al. Cellular basis for the negative inotropic effects of tumor necrosis factor-α in the adult mammalian heart. *J Clin Invest.* 1993;92:2303–2312.
22. Balligand JL, Ungureanu-Longrois D, Simmons WW, et al. Cytokine-inducible nitric oxide synthase (iNOS) expression in cardiac myocytes: characterization and regulation of iNOS expression and detection of iNOS activity in single cardiac myocytes in vitro. *J Biol Chem.* 1994; 269:27580–27588.
23. Smart SJ, Casale TB. Pulmonary epitherial cells facilitate TNF-α-induced neutrophil chemotaxis. *J Immunol.* 1994;152:4087–4094.
24. Maloff BL, Shaw JE, Fox D. A chemotaxis assay using human polymorphonuclear leukocytes stimulated by IL-1. *J Immunol Methods.* 1988; 112:145–146.
25. Riper GV, Siciliano S, Fischer PA, et al. Characterization and species distribution of high affinity GTP-coupled receptors for human Rantes and monocyte chemoattractant protein 1. *J Exp Med.* 1993;177:851–856.
26. Mori E, Komori K, Yamaoka T, et al. Essential role of monocyte chemoattractant proteine-1 in development of restenotic changes (neointimal hyperplasia and constructive remodeling) after balloon angioplasty in hypercholesterolemic rabbits. *Circulation.* 2002;105:2905–2910.